

This discussion paper is/has been under review for the journal Hydrology and Earth System Sciences (HESS). Please refer to the corresponding final paper in HESS if available.

Combining remote sensing and GIS climate modelling to estimate daily forest evapotranspiration in a Mediterranean mountain area

J. Cristóbal^{1,4}, R. Poyatos², M. Ninyerola¹, P. Llorens³, and X. Pons⁴

¹Department of Animal Biology, Plant Biology and Ecology, C-Building, Universitat Autònoma de Barcelona, Cerdanyola del Vallès, 08193, Spain

²Center for Ecological Research and Forestry Applications (CREAF), Universitat Autònoma de Barcelona, Cerdanyola del Vallès, 08193, Spain

³Institute of Environmental Assessment and Water Research (IDÆA), CSIC, Jordi Girona, 18, Barcelona, 08034, Spain

⁴Department of Geography, B-Building, Universitat Autònoma de Barcelona, Cerdanyola del Vallès, 08193, Spain

1125

Received: 13 December 2010 – Accepted: 3 January 2011 – Published: 25 January 2011

Correspondence to: J. Cristóbal (jordi.cristobal@uab.cat)

Published by Copernicus Publications on behalf of the European Geosciences Union.

where $NDVI^*$ is a scaled vegetation index based on the NDVI and is defined as:

$$NDVI^* = \frac{NDVI_p - NDVI_0}{NDVI_s - NDVI_0} \quad (4)$$

where subindex p is the image NDVI value for a given pixel, 0 is a bare soil pixel and s is a fully vegetated pixel.

5 2.4 ET_d model inputs

2.4.1 Landsat and TERRA/AQUA image processing

Landsat images were corrected by means of conventional techniques based on first order polynomials. The effect of the relief of the land surface was taken into account by using a digital elevation model (Palà and Pons, 1995), and a mean RMSE less than 10 15 m was obtained. Radiometric correction was carried out following the methodology proposed by Pons and Solé-Sugrañes (1994), which allows us to reduce the number of undesired artifacts due to the atmospheric effects or differential illumination that are results of the time of day, the location on the Earth and the relief (zones being more illuminated than others, shadows, etc). The digital numbers were converted to radiances by means of image header parameters, taking into account the considerations 15 presented by Cristóbal et al. (2004) and Chander et al. (2009).

Given that AQUA/TERRA MODIS reflectance and LST and emissivity products are corrected geometrically and radiometrically by USGS, these products were only imported, with all the necessary metadata to process them. Before that, images 20 were reprojected to UTM-31 N. The water vapour product was geometrically corrected using HEG-WIN software (<http://newsroom.gsfc.nasa.gov/sdptoolkit/HEG/HEGDownload.html>).

1133

2.4.2 Air temperature

Different air temperature input variables are needed to compute net radiation LST and ET_d : satellite pass air temperature (T_i), daily mean air temperature (T_a) and daily minimum air temperature (T_{min}). To regionalize air temperature, we applied multiple regression analysis combined with spatial interpolation techniques (Cristóbal et al., 2008; 5 Ninyerola et al., 2000, 2007). Air temperature data were fitted using 60% of the meteorological ground stations and cross-validated with the remaining 40%. In these previous works, T_i , T_a and T_{min} were obtained with an RMSE of 1.8 K, 1.3 K and 2.3 K, respectively.

10 2.4.3 Land surface temperature (LST) and emissivity (LSE)

In the case of Landsat-5 TM and Landsat-7 ETM+, the LST was calculated with the methodology proposed by Cristóbal et al. (2009), which is based on the radiative transfer equation and needs air temperature and water vapour as input variables. It yielded a RMSE of about 1 K. The methodology is designed for a wide range of water vapour values (0 to 8 g cm⁻²) to take into account global conditions. The TERRA/AQUA 15 MODIS water vapour product (MOD05) was used as the water vapour source. The air temperature was computed as explained in Sect. 2.4.2.

To compute LSE we used the NDVI threshold method proposed by Sobrino and Raisouni (2000) and Sobrino et al. (2008). This methodology uses certain NDVI thresholds 20 to distinguish between bare soil, fully vegetated and mixed pixels. According to the authors it gives an error of 1% (Sobrino et al., 2008).

2.4.4 Net radiation (R_n)

Daily net radiation was computed with the energy balance equation as follows:

$$R_n = R_{s\downarrow} \cdot (1 - \alpha) + \varepsilon_a \cdot \sigma \cdot T_a^4 - \varepsilon \cdot \sigma \cdot LST^4 \quad (5)$$

1134

3 Results and discussion

3.1 B parameter

The B parameter showed different behaviour depending on the approach used. The $B-R_n$ ratio local had a mean and standard deviation (s.d.) of 6.9 and 3.2 Wm^{-2} , respectively, in the case of Landsat dates (see Fig. 2), and a mean and s.d. of 10.8 and 2.2 Wm^{-2} , respectively, in the case of TERRA/AQUA dates. The $B-R_n$ ratio regional displayed a mean and s.d. of 9.5 and 2.3 Wm^{-2} , respectively, in the case of Landsat dates, and a mean and s.d. of 12.8 and 2.4 Wm^{-2} , respectively, in the case of TERRA/AQUA dates. Finally, B -NDVI showed a mean and σ of 11.9 and 2.6 Wm^{-2} , respectively, in the case of Landsat dates, and a mean and σ of 12.6 and 2.6 Wm^{-2} , respectively, in the case of TERRA/AQUA dates.

B -NDVI was similar in Landsat and TERRA/AQUA dates, but not in the B approach using the R_n ratio, especially in the case of the $B-R_n$ ratio local. While on winter and autumn dates the $B-R_n$ ratio local had small values (positive or negative) close to 0, B -NDVI tended to show higher positive values. For example, B computed on 11 January 2005, using the R_n local ratio gave a negative value close to 0 Wm^{-2} , whereas in the case of B -NDVI it was 11.8 Wm^{-2} . During these seasons we would expect low B values due to the energy budget; therefore, this suggests that B -NDVI could be less sensitive in winter and autumn situations than the $B-R_n$ ratio.

In the case of the $B-R_n$ ratio, the R_n ratio is usually obtained from a net radiation sensor over the study area. Some authors have used a constant value of 0.3 ± 0.02 (Seguin and Itier, 1983; Kustas et al., 1990; García et al., 2007) because most of the dates used in these studies were in spring or summer and over crop areas. However, we found that our local (Vallcebre research catchments) and regional (SMC meteorological stations) R_n ratios varied over the year (see Fig. 3). The R_n local and regional ratios for the Landsat/TERRA satellite pass had an annual mean (from 2003 to 2005 period) of 0.16 ± 0.05 (mean and s.d.) and 0.22 ± 0.03 , respectively, and in the case

1137

of the AQUA satellite pass, an annual mean of 0.17 ± 0.05 and 0.21 ± 0.02 , respectively. In addition, the R_n ratio varied little from 09:00 to 14:00 LST in our study area, and thus was useful in Landsat and TERRA/AQUA ET_d modelling. Therefore, we used a daily R_n ratio instead of a constant R_n ratio. This is in agreement with other authors who also reported a similar R_n ratio behaviour (Sánchez et al., 2007; Sobrino et al., 2005; Wassenaar et al., 2002). R_n ratio values reported in these studies are similar to the regional R_n ratio computed in our study area because our value was obtained at meteorological stations at a similar altitude as those in the literature. However, the local R_n ratio values are lower, which shows that this ratio does not only vary with latitude as Sánchez (2007) suggests, but also with altitude. Further research into R_n ratio modelling in mountainous areas is therefore needed.

Moreover, it is worth remarking that the local R_n ratio obtained in the Scots Pine stand displayed a different pattern to the regional R_n ratio because it had negative values on winter days when the R_n budget is negative, which often occurs in mountainous areas (Barry, 2001). ET_d models do not usually predict this situation because they are generally applied in spring and summer and in relatively flat and low altitude areas.

3.2 Net radiation validation

The results show a good agreement between the R_{nd} measured in the Scots Pine stand and the R_{nd} obtained using the Landsat regional model with an R^2 of 0.89 and an RMSE of 22 Wm^{-2} (see Table 1). The R_{nd} derived from TERRA/AQUA MODIS showed a similar RMSE but lower R^2 (0.77 and 0.73, respectively; Table 2). It is worth noting that the proposed R_{nd} model developed with regional variables, such as R_{sl} , LST and T_a , makes it possible to approximate this variable over large areas with a high level of accuracy.

1138

3.3 ET_d validation

3.3.1 Landsat

In the ET_d validation, we obtained a test R^2 of 0.84 when the B parameter was estimated using a regional R_n ratio computed with the SMC meteorological stations (B - R_n ratio regional), 0.84 when the B parameter was estimated using a local R_n ratio computed with the Scots pine stand meteorological station (B - R_n ratio local), and 0.82 when the B parameter was estimated using the NDVI approach, B -NDVI. It is interesting to note that for the ET_d models used, the minimum values were always negative. This mainly happens on winter dates when the R_n ratio is also negative. Therefore, on winter dates this methodology should only be used on days when the R_n budget is positive. Errors close to 1 mm day⁻¹ were obtained for the RMSE. Taking into account the range of ET_d values observed in the studied Scots Pine stand (from 0.5 to 2.7 mm day⁻¹), we cannot conclude that the model provides optimal results. When the R_{nd} ratio is negative during winter, the ET_d yields negative values and the model does not perform well. Again, it is worth noting that ET_d models are usually validated on spring or summer dates (Chiesi et al., 2002; Nagler et al., 2005, 2007; Sánchez et al., 2007, 2008; Verstraeten et al., 2005; Wu et al., 2006) when the daily R_n budget is positive. Our attempt to also estimate ET_d during autumn and winter has shown the limitations of the method and how ET_d modelling needs to be further improved, especially in forest areas.

We obtained a better mean RMSE for the different models when only those dates with a positive R_{nd} ratio were selected, which ranged from 0.5 to 0.7 mm day⁻¹ with a similar R^2 (see Tables 2–3 and Fig. 4). Of the different approaches used to compute the B parameter, the best results were obtained using the local R_n ratio and the NDVI approaches, with a RMSE of 0.5 and 0.6 mm day⁻¹, respectively, and an estimation error of about ±30%. Indeed, the regional R_n ratio yielded a higher RMSE and estimation error of about 0.7 mm day⁻¹ and ±38%, respectively; this could be explained by the differences in the R_n ratio estimation. The regional R_n ratio was computed from the

1139

data from the SMC meteorological stations, which are designed for crop assessment and are located in areas at low to medium heights (from 0 to 500 m). Our study area is located at 1250 m; therefore, the regional R_n ratio conditions are not representative of our study area. However, it is important to note that optimal R_n ratio values are difficult to obtain because it would be necessary to have a meteorological network with R_n instruments distributed at different altitudes in diverse landscapes. Moreover, R_n instruments are usually found in agrometeorological networks but not very often over forest areas. Although the two B parameter approaches (B - R_n ratio local and B -NDVI) obtained similar results, we have to take into account that the main disadvantage of the NDVI approach is the subjectivity involved in adopting the NDVI thresholds to compute NDVI*. However, if a well-balanced regional R_n ratio is not available due to limitations in the meteorological networks, the NDVI approach is preferable for computing the B parameter at regional scales. In all cases, the models tended to overestimate ET_d, showing higher values in the case of the regional R_n ratio and lower values in the case of the NDVI approach.

In this study, we are strictly comparing evapotranspiration with stand transpiration of the dominant tree species. As the understory in the studied stand is very poor, the only other contribution comes from soil evaporation, with typical rates of 0.1 to 0.5 mm day⁻¹ (Poyatos et al., 2007). These values are consistent with the systematic bias between sap flow-derived transpiration and the ET_d models (see Fig. 4).

In addition, it should be stressed that the difficulty of obtaining the effective aerodynamic resistance and the use of a constant value for the analyzed period may have introduced more variability into our analysis, and thus increased the error in the ET_d models.

3.3.2 TERRA/AQUA MODIS

TERRA and AQUA ET_d validation did not obtain the same results as Landsat (see Tables 2–3 and Figs. 5–6). In both cases, ET_d validation showed a higher RMSE, between 1.8 and 2.4 mm day⁻¹, and a low R^2 , between 0.03 and 0.07. Despite air

1140

- Bates, B. C., Kundzewicz, Z. W., Wu, S., and Palutikof, J. P.: Climate Change and Water, Technical Paper of the Intergovernmental Panel on Climate Change, IPCC Secretariat, Geneva, 2008.
- 5 Bastiaanssen, W. G. M., Meneti, M., Feddes, R. A., and Holtslag, A. A. M.: A remote sensing surface energy balance algorithm for land (SEBAL), 1. Formulation, *J. Hydrol.*, 212–213, 198–212, 1998.
- Carlson, T. N., Caphart, J., and Gillies, R. R.: A new look at the simplified method for remote sensing of daily evapotranspiration, *Remote Sens. Environ.*, 54, 161–167, 1995.
- Caselles, V., Sobrino, J. A., and Coll, C.: On the use of satellite thermal data for determining evapotranspiration in partially vegetated areas, *Int. J. Remote Sens.*, 13, 2669–2682, 1992.
- 10 Caselles, V., Artiago, M. M., and Hurtado, E.: Mapping actual evapotranspiration by combining Landsat and NOAA-AVHRR images: application to the Barrax area, Albacete, Spain, *Remote Sens. Environ.*, 63, 1–10, 1998.
- Chander, G., Markham, B. L., and Helder, D. L.: Summary of current radiometric calibration coefficients for Landsat MSS, TM, ETM+, and EO-1 ALI sensors, *Remote Sens. Environ.*, 15 113, 893–903, 2009.
- Chiesi, M., Maselli, F., Bindi, M., Fibbi, L., Bonora, L., Raschi, A., Tognetti, R., Cermak, J., and Nadezhdina, N.: Calibration and application of FOREST-BGC in a Mediterranean area by the use of conventional and remote sensing data, *Ecol. Model.*, 154, 251–262, 2002.
- 20 Cristóbal, J., Pons, X., and Serra, P.: Sobre el uso operativo de Landsat-7 ETM+ en Europa, *Rev. Teledetección*, 21, 55–59, 2004.
- Cristóbal, J., Pons, X., and Ninyerola, M.: Modelling actual evapotranspiration in Catalonia (Spain) by means of remote sensing and geographical information systems, *Göttinger Geogr. Abh.*, 113, 144–150, 2005.
- 25 Cristóbal, J., Ninyerola, M., and X. Pons: Modelling air temperature through a combination of Remote Sensing and GIS data, *J. Geophys. Res.*, 13, D13106, 1–13, 2008.
- Cristóbal, J., Jiménez-Muñoz, J. C., Sobrino, J. A., Ninyerola, M., and Pons, X.: Improvements in land surface temperature retrieval from the landsat series thermal band using water vapour and air temperature, *J. Geophys. Res.*, 114, D08103, 1–16, 2009.
- 30 Dilley, A. C. and O'Brien, D. M.: Estimating downward clear sky long-wave irradiance at the surface from screen temperature and precipitable water, *Q. J. Roy. Meteor. Soc.*, 124, 1391–1401, 1998.

- Gallart, F., Llorens, P., Latron, J., and Regués, D.: Hydrological processes and their seasonal controls in a small Mediterranean mountain catchment in the Pyrenees, *Hydrol. Earth Syst. Sci.*, 6, 527–537, doi:10.5194/hess-6-527-2002, 2002.
- García, M., Villagarcía, L., Contreras, S., Domingo, F., and Puigdefábregas, J.: Comparison of three operative models for estimating the surface water deficit using ASTER reflective and thermal data, *Sensors*, 7, 860–883, 2007.
- 5 Giorgi, F., Bi, X. Q., and Pal, J.: Mean interannual variability and trends in a regional climate change experiment over Europe, II: Climate change scenarios (2071–2100), *Clim. Dynam.*, 23, 839–858, 2004.
- 10 Granier, A.: Une nouvelle méthode pour la mesure du flux de sève brute dans le tronc des arbres, *Ann. Sci. Forest*, 42, 193–200, 1985.
- Hargreaves, G. H. and Samani, Z. A.: Estimating potential evapotranspiration, *J. Irr. Drain. Div.-ASCE*, 108, 225–230, 1982.
- Jackson, R. B., Carpenter, S. R., Dahm, C. N., McKnight, D. M., Naiman, R. J., Postel, S. L., and Running, S. W.: Water in a changing world, *Ecol. Appl.*, 11, 1027–1045, 2001.
- 15 Jackson, R. D., Reginato, R. J., and Idso, S. B.: Wheat canopy temperature: a practical tool for evaluating water requirements, *Water Resour. Res.*, 13, 651–656, 1977.
- Jung, M., Reichstein, M., Ciais, P., Seneviratne, S. I., Sheffield, J., Goulden, M. L., Bonan, G., Cescatti, A., Chen, J., Jeu, R., Dolman, A. J., Eugster, W., Gerten, D., Gianelle, D., Gobron, N., Heinke, J., Kimball, J., Law, B. E., Montagnani, L., Mu, Q., Mueller, B., Oleson, K., Papale, D., Richardson, A. D., Rouspard, O., Running, S., Tomelleri, E., Viovy, N., Weber, U., Williams, C., Wood, E., Zaehle, S., and Zhang, K.: Recent decline in the global land evapotranspiration trend due to limited moisture supply, *Nature*, 467, 951–954, 2010.
- Kustas, W. P. and Norman, J. M.: Use of remote sensing for evapotranspiration monitoring over land surfaces, *Hydrolog. Sci. J.*, 41, 495–516, 1996.
- 25 Kustas, W. P. and Norman, J. M.: A two-source energy balance approach using directional radiometric temperature observations for sparse canopy covered surfaces, *Agron. J.*, 92, 847–854, 2000.
- Kustas, W. P., Moran, M. S., Jackson, R. D., Gay, L. W., Duell, L. F. W., Kunkel, K. E., and Matthias, A. D.: Instantaneous and daily values of the surface energy balance over agricultural fields using remote sensing and reference field in an arid environment, *Remote Sens. Environ.*, 32, 125–141, 1990.
- 30

- Lagouarde, J. P. and Brunet, Y.: A simple model for estimating the daily upward longwave surface radiation flux from NOAA-AVHRR data, *Int. J. Remote Sens.*, 14, 907–925, 1983.
- Latron, J., Llorens, P., Soler, M., Poyatos, R., Rubio, C., Muzylo, A., Martínez-Carreras, N., Delgado, J., Regüés, D., Catari, G., Nord, G., and Gallart, F.: Hydrology in a Mediterranean mountain environment – the Vallcebre research basins (northeastern Spain), I. 20 years of investigations of hydrological dynamics. In *Status and Perspectives of Hydrology in Small Basins*, IAHS Publ. 336, IAHS Press, Wallingford, UK, 38–44, 2010.
- Liang, S.: Narrowband to broadband conversions of land surface albedo, *Remote Sens. Environ.*, 76, 213–238, 2001.
- Liang, S., Strahler, A. H., and Walthall, C.: Retrieval of land surface albedo from satellite observations: a simulation study, *J. Appl. Meteorol.*, 38, 712–725, 1999.
- Liu, J., Williams, J. R., Zehnder, A. J. B., and Yang, H.: GEPIC – modelling wheat yield and crop water productivity with high resolution on a global scale, *Agr. Syst.*, 94, 478–493, 2007.
- Llorens, P., Poyatos, R., Muzylo, A., Rubio, C., Latron, J., Delgado, J., and Gallart, F.: Hydrology in a Mediterranean mountain environment – the Vallcebre research basins (Northeastern Spain), III. Vegetation and water fluxes, in: *Status and Perspectives of Hydrology in Small Basins*, IAHS Publ. 336, IAHS Press, Wallingford, UK, 186–191, 2010.
- Mu, Q., Heinsch, F. A., Zhao, M., and Running, S. W.: Development of a global evapotranspiration algorithm based on MODIS and global meteorology data, *Remote Sens. Environ.*, 111, 519–536, 2007.
- Nadezhkina, N., Čermák, J., and Ceulemans, R.: Radial patterns of sap flow in woody stems of dominant and understory species: scaling errors associated with positioning of sensors, *Tree Physiol.*, 22, 907–918, 2002.
- Nagler, P., Cleverly, J., Glenn, E., Lampkin, D., Huete, A., and Wan, Z.: Predicting riparian evapotranspiration from MODIS vegetation indices and meteorological data, *Remote Sens. Environ.*, 94, 17–30, 2005.
- Nagler, P., Jetton, A., Fleming, J., Didan, K., Glenn, E., Erker, J., Morino, K., Milliken, J., and Gloss, S.: Evapotranspiration in a cottonwood (*Populus frmontii*) restoration plantation estimated by sap flow and remote sensing methods, *Agr. Forest Meteorol.*, 144, 95–110, 2007.
- Ninyerola, M., Pons, X., and Roure, J. M.: A methodological approach of climatological modelling of air temperature and precipitation through GIS techniques, *Int. J. Climatol.*, 20, 1823–1841, 2000.

- Ninyerola, M., Pons, X., and Roure, J. M.: Objective air temperature mapping for the Iberian Peninsula using spatial interpolation and GIS, *Int. J. Climatol.*, 27(9), 1231–1242, 2007.
- Norman, J. M., Kustas, W. P., and Humes, K.: A two-source approach for estimating soil and vegetation energy fluxes from observations of directional radiometric surface temperature, *Agr. Forest Meteorol.*, 77, 263–293, 1995.
- Oak Ridge National Laboratory Distributed Active Archive Center (ORNL DAAC): SAFARI 2000 Web Page, available at: <http://daac.ornl.gov/S2K/safari.html>, last access: 1 September, 2010.
- Oki, T. and Kanae, S.: Global hydrological cycles and world water resources, *Science*, 313, 1068–1072, 2006.
- Page, J. K.: Prediction of solar radiation on inclined surfaces, *Solar energy, R & D in the European Community, Series F: Solar Radiation Data*, 3, Reidel Publishing Company, Dordrecht, 1986.
- Palà, V. and Pons, X.: Incorporation of relief into geometric corrections based on polynomials, *Photogramm. Eng. Rem. S.*, 61, 935–944, 1995.
- Pons, X. and Ninyerola, M.: Mapping a topographic global solar radiation model implemented in a GIS and refined with ground data, *Int. J. Climatol.*, 28, 1821–1834, 2008.
- Pons, X. and Solé-Sugrañes, L.: A simple radiometric correction model to improve automatic mapping of vegetation from multispectral satellite data, *Remote Sens. Environ.*, 47, 1–14, 1994.
- Poyatos, R., Latron, J., and Llorens, P.: Land-use and land-cover change after agricultural abandonment, The case of a Mediterranean Mountain Area (Catalan Pre-Pyrenees), *Mt. Res. Dev.*, 23, 52–58, 2003.
- Poyatos, R., Llorens, P., and Gallart, F.: Transpiration of montane *Pinus sylvestris* L. and *Quercus pubescens* Willd. forest stands measured with sap flow sensors in NE Spain, *Hydrol. Earth Syst. Sci.*, 9, 493–505, doi:10.5194/hess-9-493-2005, 2005.
- Poyatos, R., Villagarcía, L., Domingo, F., Piñol, J., and Llorens, P.: Modelling evapotranspiration in a Scots Pine stand under Mediterranean mountain climate using the GLUE methodology, *Agr. Forest Meteorol.*, 146, 13–28, 2007.
- Poyatos, R., Llorens, P., Piñol, J., and Rubio, C.: Response of Scots Pine (*Pinus sylvestris* L.) and pubescent oak (*Quercus pubescens* Willd.) to soil and atmospheric water deficits under Mediterranean mountain climate, *Ann. Forest Sci.*, 65, 306, 2008.

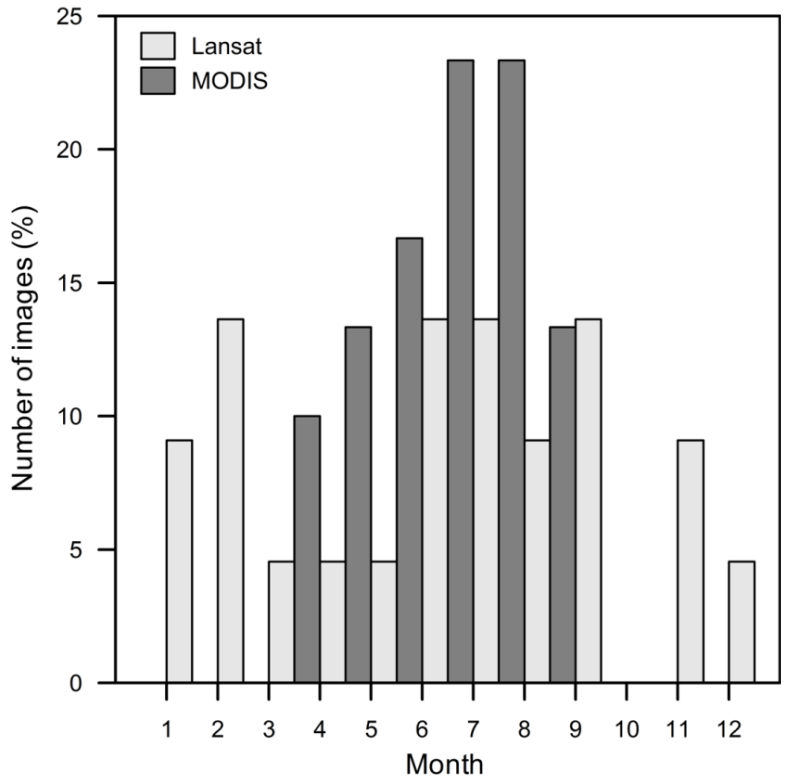


Fig. 2. Monthly temporal distribution of satellite data (clear sky and without bow tie effect) used during the period 2003–2005.

1155

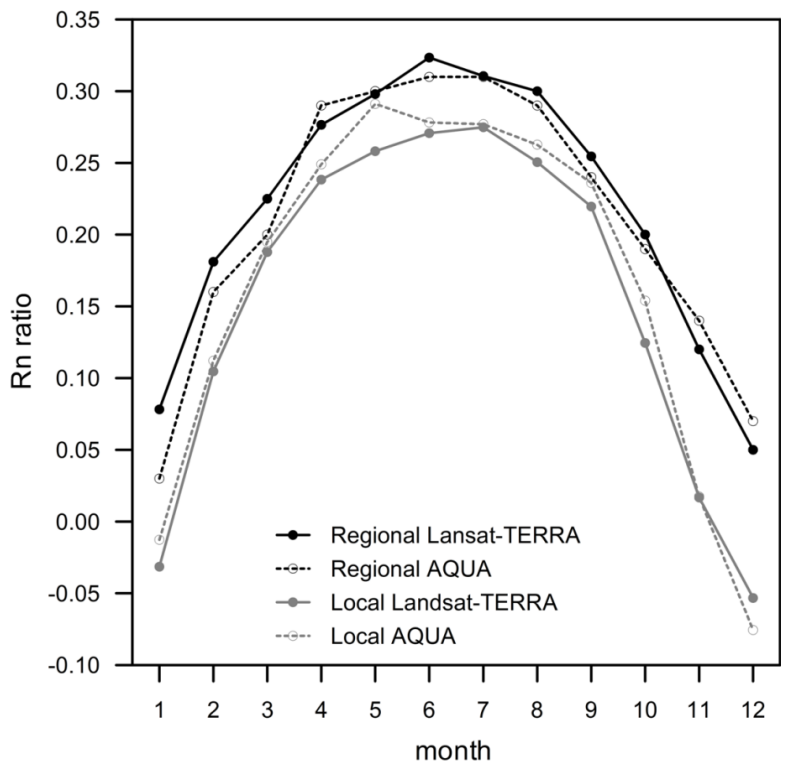


Fig. 3. Mean monthly local and regional R_n at the Landsat/TERRA and AQUA satellite pass on clear sky days from 2003 to 2005.

1156

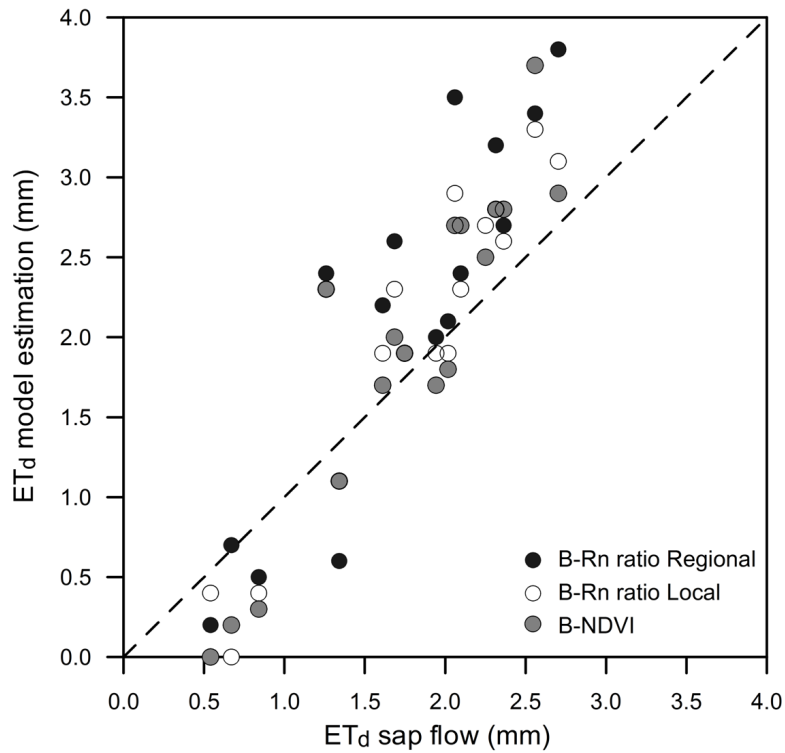


Fig. 4. Relationship between daily evapotranspiration (ET_d) calculated from sap flow measurements modelled using Landsat data and the B parameter approach in $mm\ day^{-1}$. B - R_n ratio regional is the B approach using the regional R_n ratio, B - R_n ratio local is the B approach using the local R_n ratio and B -NDVI is the B approach using the NDVI.

1157

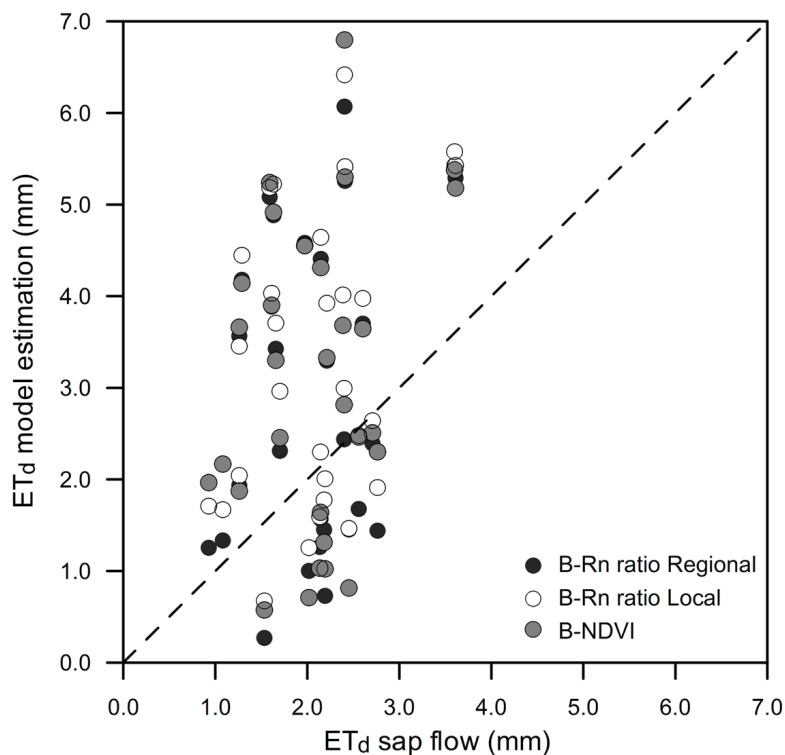


Fig. 5. Relationship between daily evapotranspiration (ET_d) calculated from sap flow measurements and modelled using TERRA MODIS data and the B parameter estimation in $mm\ day^{-1}$. B - R_n ratio regional is the B approach using the regional R_n ratio, B - R_n ratio local is the B approach using the local R_n ratio and B -NDVI is the B approach using the NDVI.

1158

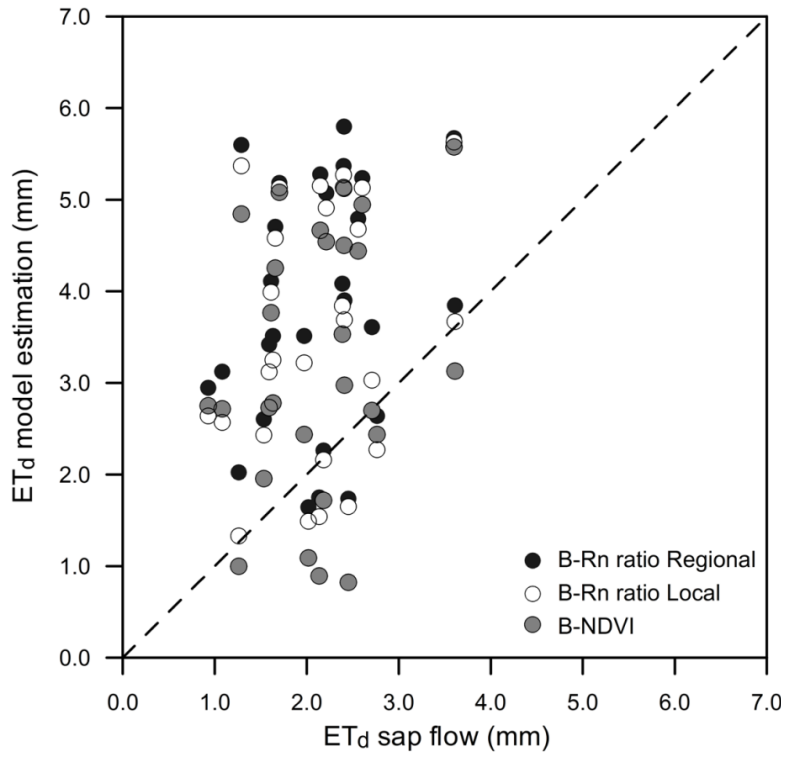


Fig. 6. Relationship between daily evapotranspiration (ET_d) calculated from sap flow measurements and modelled using AQUA MODIS data and the B parameter estimation in $mm\ day^{-1}$. $B-R_n$ ratio regional is the B approach using the regional R_n ratio, $B-R_n$ ratio local is the B approach using the local R_n ratio and $B-NDVI$ is the B approach using the NDVI.